Selenate bioreduction in a large in situ field trial

M. Jim Hendry, Lisa Kirk, Jeff Warner, Shannon Shaw, Brent Peyton, Erin E. Schmeling, S. Lee Barbour

SELENATE BIOREDUCTION IN A LARGE *IN SITU* FIELD TRIAL

M. Jim Hendry[1], Lisa Kirk[2], Jeff Warner[3], Shannon Shaw[4], Brent M. Peyton[5], Erin Schmeling[1], and S. Lee Barbour[6]

[1]Department of Geological Sciences, University of Saskatchewan, 114 Science Place, Saskatoon, SK, S7N 5E2, Canada *(e-mail: jim.hendry@usask.ca; erin.schmeling@usask.ca)*

[2] Enviromin, Inc. 524 Professional Drive, Bozeman, MT, 59715, USA (*e-mail: lisakirk@enviromininc.com)*

[3] Canadian Light Source Inc., University of Saskatchewan, 101 Perimeter Road, Saskatoon, SK, Canada S7N 0X4; Now with Ensero Solutions, 104-411 Downey Rd., Saskatoon, SK, S7N 4L8 (*e-mail*: *jwarner@ensero.com*)

[4]SRK Consulting, 1066 W. Hastings St., Vancouver, BC, V6E 3X2, Canada (*e-mail: SShaw@SRK.com*)

[5] Department of Chemical and Biological Engineering, Center for Biofilm Engineering, 305 Cobleigh Hall, Montana State University, Bozeman, MT, USA (*e-mail: bpeyton@montana.edu*)

[6]Department of Civil and Geological Engineering, University of Saskatchewan, 57 Campus Drive, Saskatoon, SK, S7N 5A9, Canada *(deceased)*

Abstract:
Removing selenium (Se) from mine effluent is a common challenge. A long-term, *in situ* experiment was conducted to bioremediate large volumes (up to 7500 m^3 d^{-1}) of Se(VI)-contaminated water (mean 87 µg L^{-1}) by injecting the water into a saturated waste rock fill (SRF) at a coal mining operation in Elk Valley, British Columbia, Canada. To stimulate/maintain biofilm growth in the SRF, labile organic carbon (methanol) and nutrients were added to the water prior to its injection. A conservative tracer (Br^-) was also added to track the migration of injected water across the SRF, identify wells with minimal dilution and used to quantify the extent of bioreduction. The evolution of the Se species through the SRF was monitored in time and space for 201 d. Selenium concentrations of <3.8 µg L^{-1} were attained in monitoring wells located 38 m from the injection wells after 114 to 141 d of operation. Concentrations of Se species in water samples from complementary long-term (351-498 d) column experiments using influent Se(VI) concentrations of 1.0 mg L^{-1} were consistent with the results of the *in situ* experiment. Solid samples collected at the completion of the column experiments confirmed the presence of indigenous Se-reducing bacteria and that the sequestered Se was present as insoluble Se(0), likely in Se-S ring compounds. Based on the success of this ongoing bioremediation experiment, this technology is being applied at other mine sites.

Keywords: Selenium, Selenium Speciation, Bioreduction, Microbial Ecology, XANES, Denitrification, Mining

Synopsis: *In situ* bioreduction successfully removes selenium and nitrate from large volumes of mine-contaminated water.

Highlights

- Selenium originating from weathering of coal mine waste rock can contaminate receiving waters.
- A large-scale, *in situ* bioremediation experiment successfully removed dissolved selenate (mean = 87 µg L^{-1}) from large volumes of mine water (up to 7500 m^3 d^{-1}) over a 201-d study period.
- Complimentary column experiments confirmed selenate reduction to insoluble Se(0) via indigenous selenium-reducing bacteria.
- Monitoring well and column data show that nitrate and selenium are concurrently reduced with no observed inhibition of selenium reduction by nitrate.

53 **TOC/ABSTRACT ART**

54

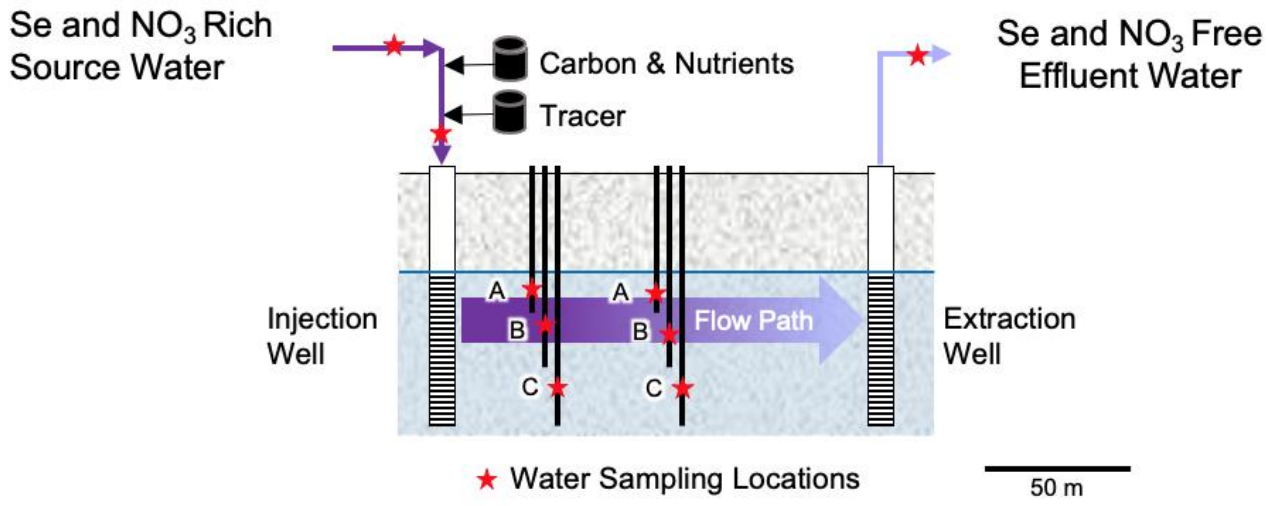

55

1. INTRODUCTION

Selenium (Se) is an essential element for living organisms but can be toxic even at low concentrations (Lenz and Lens 2009; Lemly, 1993). Due to its toxicity, Health Canada (2014) and the United States Environmental Protection Agency (US EPA, 2009) stipulate a drinking water standard for Se of 50 µg L^{-1} and the United States Environmental Protection Agency (US EPA, 2021) and the province of British Columbia (B.C., 2023) stipulate a monthly average aquatic limit of 3.1 and 2.0 µg L^{-1}, respectively. Selenium in aquatic environments can be derived from both natural and anthropogenic sources. Natural sources of Se include volcanic activity and rock weathering. Anthropogenic sources include increasing rates of release from rock weathering during coal mining (cf., Griffith et al., 2012; Lindberg et al., 2011; Hendry et al., 2015), base metal mining, milling and smelting (ATSDR, 2003), and petrochemical and industrial manufacturing operations, as well as irrigation of Se-rich soils (Lemly, 1993).

Selenium concentrations in the Elk River have exceeded the B.C. water quality guideline of 2 µg/L total Se at the town of Elko approximately 60 km south of Sparwood (Fig. 1) since the late 1990s (Beatty and Russo, 2014; Swanson, 2010). The Se in the Elk River upstream of Elko is attributed to the oxidation of Se-bearing sulfide minerals in large waste rock dumps located at steelmaking coal mining operations throughout the valley (McDonald and Strosher, 1998; Wellen et al., 2015; Dessouki and Ryan, 2010; Kennedy et al., 2000; Storb et al. 2023) (Fig. 1). Selenium bioreduction has been identified as an important Se removal mechanism in suboxic and anaerobic environments (*cf.,* Bianchin et al., 2013; Boltz and

79 Rittman, 2021; Deen et al., 2018; Kirk, 2014; Lai et al., 2020). Se bioreduction
80 occurs in natural marsh and oxbow settings in the Elk Valley (Martin et al., 2011),
81 and *in situ* Se(VI) bioreduction can be effective in controlling Se concentrations in
82 suboxic zones in unsaturated (Kennedy et al., 2015) and water-saturated (Bianchin
83 et al., 2013) coal waste rock. Based in part on these findings, a large-scale, multi-
84 year bioremediation experiment was conducted to investigate the effectiveness of
85 the *in situ* bioreduction of dissolved Se(VI) from large volumes of Elk Valley mine
86 water (up to 7,500 $m^3 d^{-1}$). Mine water was injected together with a labile organic
87 carbon source and nutrients into a saturated rock fill (SRF) hosting native nitrate
88 (NO_3^-)- and Se-reducing microbes. The evolution of the Se through the SRF was
89 monitored over time and space. The field-based study was augmented with
90 laboratory column experiments to simulate the Se(VI) bioreduction process in the
91 SRF and provide insights into the indigenous microorganisms responsible for the
92 Se(VI) bioreduction and the mineralogical end point of the bioreduced Se.
93 The mine water injected into the SRF also contained elevated concentrations of
94 mining-derived NO_3^-. In a companion paper, Hendry et al. (2023) show the NO_3^-
95 in the large volumes of injected water (mean 22±5.7 mg N L^{-1}) is denitrified in the
96 SRF. Literature on the potential for NO_3^- inhibition of Se bioreduction is conflicting.
97 Some studies demonstrate elevated NO_3^- concentrations inhibit Se(VI) reduction
98 in both field and laboratory test conditions (*cf.,* Bailey et al., 2012; Gates et al.,
99 2009). In contrast, other laboratory and field studies show simultaneous reduction
100 of NO_3^- and Se(VI) (*cf*., Bianchin et al., 2013; Macy et al., 1993; Oremland et al.,
101 1999). Thus, in addition to characterizing the *in situ* bioreduction of dissolved

102 Se(VI), the current study provides an opportunity to assess the inhibition of Se
103 bioreduction by NO_3^- at the field and column scales for the concentrations tested.

104 **2. METHODS**

105 2.1 Field Experiment

106 The *in situ* bioremediation experiment was conducted in the F2-SRF at the Elkview
107 Operations (EVO) located in the Elk Valley, British Columbia, Canada (Fig. 1a and
108 b). The SRF is filled with waste rock (*i.e.,* earth materials overlying the coal
109 deposits excavated during open-pit mining activities). This SRF is about 350 m
110 wide × 800 m long × 130 m thick, with a saturated zone (~20 to 84 m thick)
111 containing ~2.7 M m^3 of water that is overlain by 60 to 80 m of unsaturated waste
112 rock.

113 Three injection and extraction wells were installed in rows in the SRF (Fig. 1c). The
114 extraction wells were installed ~150 m from the injection wells, and two rows of
115 nested monitoring wells were installed parallel to and between the injection and
116 extraction wells. The nested monitoring wells were located about 35 m (Row 1)
117 and 75 m (Row 2) from the injection wells. Monitoring well nests 01 to 04 were in
118 Row 1 and 05 to 09 were in Row 2. Each nest consisted of between two and five
119 wells labelled A to E, with the screen intake for A being the shallowest (located at
120 the water table) and E the deepest (located at or near the base of the SRF).

121 The bioremediation experiment was initiated on January 11, 2018 (day 1) by
122 injecting Se- and NO_3^--rich mine water into a zone 10 to 24 m below the water
123 table via the injection wells. A conservative tracer (Br^-) was continually added to

124 the injection water starting on day 1. Hendry et al. (2023) report uncertainty in the
125 Br^- dosing concentrations until day 6. Methanol was added to the injection water
126 starting on day 6 to provide a labile source of carbon and energy for microbial
127 growth and reduction of NO_3^- and Se. Hendry et al. (2023) report a blockage of
128 the methanol line at injection well (IW)-02 was not resolved until day 19 and, as a
129 result, the injection concentrations of methanol prior to day 19 are not known. The
130 average methanol dose per day for the first 201 days of the experiment was 511 L
131 d^{-1} corresponding to an average COD:N of 6.5 and concentration of 33 mg L^{-1} as
132 dissolved organic carbon (DOC). Based on results of preliminary batch tests (data
133 not provided), yeast extract was added to the influent to provide phosphorous (P)
134 at a target concentration of ~0.1 mg P L^{-1}. Yeast extract addition was started at a
135 low concentration on day 29 and increased to the target concentration on day 49
136 to support cell growth and activity. The average dose added for the first 201 days
137 was 120 L d^{-1} corresponding to an average concentration of yeast extract of 6 mg
138 L^{-1} of which 2%, or 0.1 mg P L^{-1}, was present as P. The yeast extract also provided
139 some additional carbon and trace nutrients to support the initial growth phase.

140 To allow the Se chemistry results presented in this paper to be correlated with the
141 NO_3^- results presented in Hendry et al. (2023), the experimental time period and
142 the monitoring wells studied in the current study were the same as those used in
143 Hendry et al. (2023). Specifically, their study addressed the evolution of
144 denitrification in the SRF from start up to day 201. Further, to assess the evolution
145 of the injected NO_3^- in the SRF without addressing the effects of mixing of multiple
146 sources of water (and dissolved chemistry), the Hendry et al. (2023) study was

147 limited to monitoring well waters that yielded Br^- tracer concentrations that were
148 very similar to the injected concentrations (*i.e.,* the same Br^- concentrations). Wells
149 that met this criterion were the A level monitoring wells 01A, 02A, 03A, 06A, and
150 07A; these wells are thus the focus of this study as well. The pump depths in these
151 A level wells were typically 0 to 5 m below the water table.

152 Throughout the study period, the volumetric flow rate of water extracted from the
153 extraction wells was the same as that injected in the injection wells. An injection-
154 withdrawal flow rate of 5,000 $m^3\ d^{-1}$ was established on day 1. On day 174 the flow
155 rates were increased to 7,500 $m^3\ d^{-1}$ and maintained at this flow rate for the
156 remainder of the study period. From day 1 to 27, the extracted water was recycled
157 into the source reservoir. After day 28, the extracted water was discharged to the
158 environment following testing for compliance with water quality criteria. Over the
159 study period, approximately 931,000 m^3 of Se- and NO_3^--rich water was injected
160 into the SRF. The SRF was operated continuously except when system-wide
161 shutdowns occurred from day 91 to 99 and day 127 to 129.

162 Many of the laboratory methods used to meet the objectives of the current study
163 were used in the companion paper on denitrification (Hendry et al., 2023) and
164 described therein. For completeness, key methods are described below.

165 Limited water samples were collected from the monitoring wells prior to start up
166 (between August 03, 2017 and December 29, 2017). After start up, water samples
167 were collected daily from injection wells and at 2 to 4 d intervals from monitoring
168 wells. Dissolved oxygen (DO), temperature, pH, oxidation-reduction potential

169 (ORP), and conductivity were measured in the field. Aqueous samples were
170 analyzed for anions, cations, and trace metals/metalloids at ALS Environmental,
171 Calgary, AB, Canada. The dissolved species reported in this study include Br^-,
172 NO_3^--N, methanol (presented as DOC), and Se. Dissolved Se concentrations were
173 analyzed using the SW6020A method (US EPA, 1998). The lower limit of detection
174 (LLD) was 0.25 mg L^{-1}, 0.025 mg L^{-1}, 0.5 mg L^{-1}, and 0.1 µg L^{-1} for dissolved Br^-,
175 NO_3^--N, DOC, and Se analyses, respectively. Measured values are reported here
176 as mean and standard deviations where possible.

177 Water samples were collected every 6 to 8 d from the monitoring and injection
178 wells for Se speciation analyses starting on day 36 and 70, respectively. Samples
179 collected for total and dissolved Se analyses were collected in 125-mL glass
180 bottles. The samples for total Se were not filtered while those for dissolved Se were
181 filtered in the field (0.45 µm). Both total and dissolved Se samples were preserved
182 with nitric acid and stored at 4 °C. Another set of samples collected for Se
183 speciation analyses was field filtered (also 0.45 µm) into 125-mL HDPE bottles,
184 frozen immediately, and analyzed by Brooks Applied Labs (Bothell, WA, USA).
185 Dissolved Se species were analyzed using US EPA Method E1638M. The LLD for
186 dissolved Se samples was typically 0.05 µg L^{-1}. Ion chromatography inductively
187 coupled plasma collision reaction cell mass spectrometry (IC-ICP-CRC-MS)
188 analyses were used to measure Se(VI), Se(IV), methylseleninic acid (MeSe(IV)),
189 selenocyanate (SeCN), selenomethionine (SeMe), selenosulfate ($SeSO_3$),
190 dimethylselenoxide (DMSeO), and unknown selenium species with LLD values for
191 these analyses of 0.015, 0.015, 0.005, 0.015, 0.005, 0.015, 0.005 and 0.015 µg

192 L^{-1}, respectively. After day 100, the LLD values were modified to 0.06, 0.06, 0.01,
193 0.04, 0.01, 0.06, 0.01 and 0.06 µg L^{-1}, respectively.

194 Microbial communities from the SRF field experiment (data not presented) were
195 characterized every three months during SRF operation using the same methods
196 applied for characterization of microbial communities from laboratory columns
197 described below.
198

199 2.2 Column Experiments

200 Column experiments were conducted in triplicate columns (columns 9, 10, and 12)
201 to confirm NO_3^- and Se(VI) bioreduction under conditions consistent with those in
202 the SRF field experiment. Each column was constructed using a split of a
203 representative composite of waste rock with native microbes and operated in the
204 same manner. Columns 9 and 10 were operated for 498 d. Column 12 was
205 operated as a reserve column and was destructively sampled after 281 d for
206 mineralogical analysis of Se sequestration products and microbiological analyses.
207 All column tests were conducted at a field-relevant temperature (8±2 °C) in
208 sterilized stainless-steel columns (0.1 m dia. × 0.60 m high) by Enviromin Inc.
209 (Bozeman, MT, USA). Each column was loaded with 4.82 kg of composited <25
210 mm diameter waste rock fragments collected from the SRF via sonic drilling and
211 preserved under aseptic conditions in an anoxic environment (N_2 atmosphere).
212 SRF water was amended with Se(VI) to yield influent concentrations of 1.0 mg L^{-1}
213 Se(VI) as Se (about an order of magnitude greater than the mean of the injected
214 water in the field experiment of 87±31 µg L^{-1}).The initial SRF water NO_3^-

concentration was 30 mg NO_3-N L^{-1} (slightly greater than the mean of the longer term injected water in the field experiment of 22±5.7 mg N L^{-1}). Over the duration of the column tests, as water supplies were replaced, NO_3^- was amended to maintain the initial SRF concentration. Nitrate and Se(VI) bioreduction were stimulated by adding methanol at a COD:N ratio of 3.8 (or 28.5 mg L^{-1} as DOC) to the injection water, similar to the concentrations observed in the field experiment. Yeast extract was replaced with phosphoric acid at 0.09 mg P L^{-1} in the column experiments. The amended water was sparged with N_2 gas to remove oxygen and injected into the column in an upward flow configuration at 1.2 L d^{-1}. Columns were operated for approximately six months before the start of this test to build biomass and stabilize the column systems.

Weekly samples were collected from columns 9 and 10 for analysis of parameters including, but not limited to DOC (LLD 1.5 mg L^{-1}), NO_3^--N (LLD 0.23 mg L^{-1}using Hach™ spectrophotometry kits. Dissolved oxygen (LLD 2%), pH (LLD 0.1 s.u.) and ORP (LLD 10 mV) were also measured weekly in the effluent using a YSI-Proplus Multiparameter with Pro series Quattro Sonde™. Dissolved Se was analyzed by Energy Laboratories (Billings, MT, USA) via ICP-MS following US EPA method 200.8 (1994) (LLD 0.001 mg L^{-1}), and Se species were analyzed monthly at Brooks Applied Labs as described above. Because column 12 was operated in an identical fashion to the other two columns and as a reserve column, it was not monitored routinely; Se concentrations were, however, monitored infrequently to confirm reduction using the same analytical methods as for columns 9 and 10.

237 Solid samples were collected during the decommissioning of the columns for
238 microbial (columns 9 and 10) and mineralogical (column 12) analyses. Three solid
239 samples (25 g) were collected aseptically from each of columns 9 and 10 at
240 distances of 0, 0.1 and 0.3 m from the influent end of the column for microbial
241 analysis. These samples were preserved immediately in DNA/RNA Shield™
242 (Zymo Research, Irvine, CA). DNA was extracted and purified from the samples
243 using a FastDNA Spin Kit for Soils (MP Biomedicals, Irvine, CA) following the
244 manufacturer's instructions. The DNA extracts were quantified fluorometrically
245 using a Qubit dsDNA HS Assay kit (Invitrogen, Waltham, MA) and then submitted
246 to the Integrated Microbiome Resource (Dalhousie University, Halifax, NS,
247 Canada) where the V6-V8 region of the 16s rRNA gene was PCR amplified in
248 duplicate using bacterial specific fusion primers 969F and 1406R, with Illumina
249 adapters and indices attached (Comeau et al., 2011). The duplicate PCR products
250 were pooled, cleaned, and normalized using a high-throughput Charm Biotech
251 Just-a-Plate 96-well Normalization Kit (Charm Biotech, San Diego, CA) then
252 sequenced using Illumina MiSeq 2x300 bp paired-end technology. Demultiplexed
253 sequences were quality checked and primers removed using *cutadapt* (Martin,
254 2011) implemented in Python 3. After reads were filtered to remove low quality
255 reads, sequencing errors assessed, reads merged, and chimeric sequences
256 removed, taxonomy was assigned using dada2 (Callahan et al., 2016)
257 implemented in R. The publicly available SILVA reference database (v138.1) was
258 used to assign taxonomy down to the species level, where available. Functional
259 predictions were made using the FAPROTAX 1.2.6 (Louca et al., 2016) database

with updated annotations added for nitrate reducing and selenium reducing bacteria (Nancharaiah et al., 2015).

Duplicate solid samples (25 g) were collected aseptically at distances of 0, 0.1 and 0.3 m from the influent end of column 12 for mineralogical analyses. The first set of solid samples was placed in sterile 50 mL polypropylene conical tubes and into a dry ice/ethanol bath for 10 min. The tubes were then transferred into a −20 °C freezer. The second set of subsamples was dried in a N_2 environment. In addition to samples collected during deconstruction of the columns, samples were collected to define baseline conditions; specifically, one sample of pre-test waste rock used to construct the column was dried and used to characterize baseline mineralogy. Mineralogy samples were shipped frozen to the University of Saskatchewan Department of Geological Sciences (U of S; Saskatoon, SK, Canada) where they were received in a frozen state. The first set of (dried) subsamples were submitted to ALS Environmental (Saskatoon, SK, Canada) where they were disaggregated and sieved. The metals/metalloids in the <2 mm size fraction were solubilized by heated digestion with nitric and hydrochloric acids using the 200.2/6020A method and analyzed via ICPMS (US EPA, 1998). The method detection limit for Se using this method was 0.20 mg kg^{-1}. The second set of duplicate mineralogy samples was immediately taken to the Canadian Light Source (CLS, Saskatoon, SK, Canada) where they were stored in a −80 °C freezer until analyzed by X-ray absorption near-edge structure (XANES) spectroscopy. Se K-edge XANES spectra were collected on the BioXAS-spectroscopy (07ID-2) beamline on all solid subsamples and nine reference compounds (Table S1). BioXAS uses a 2.1 T

283 wiggler and a double-crystal Si (220) monochromator with a Rh-coated mirror to
284 deliver an X-ray beam in the spectral range from 5 to 32 keV. Sample spectra were
285 collected in fluorescence mode using two 32-element Ge detectors mounted in
286 plane with the sample and perpendicular to the X-ray beam. The processing of
287 spectra, including energy calibration, background subtraction, and normalization,
288 was performed using the Athena program in the Demeter package (version 0.9.26)
289 (Ravel and Newville, 2005).

290 **3. RESULTS AND DISCUSSION**

291 3.1 Field Experiment

292 *3.1.1 Injected Water Chemistry*

293 The mean pH, DO, and ORP of the injection water were 7.2±0.2, 5.3±2.5 mg L^{-1},
294 and 78.9±49.7 mV, respectively. The mean ± standard deviation of pre-test pH,
295 DO, and ORP from the monitoring wells representing background pit water
296 chemistry were 6.8±0.1, 0.3±0.7 mg L^{-1}, and 34.1±43.9 mV, respectively.

297 The mean dissolved Se and NO_3^- concentrations in the water injected into the SRF
298 were 87±31 µg L^{-1} (n=143) and 22±5.7 mg N L^{-1} (n=188), respectively. The
299 dissolved Se and NO_3^- concentrations in the injected water both varied with time
300 (Fig. 2a and 2b). In the case of Se, it decreased from 144 to 38 µg L^{-1} from day 1
301 to 43, then increased to 166 µg L^{-1} on day 114, decreased to ~44 µg L^{-1} on day
302 145, and increased to ~95 µg L^{-1} from day 195 to the end of the trial (day 201).
303 The NO_3^- concentrations decreased from ~30 to 9 mg N L^{-1} from day 1 to 43 then
304 increased to 33 mg N L^{-1} on day 79 and then decreased to ~24 mg N L^{-1} on day
305 110 and thereafter remained relatively constant. The trends in both dissolved Se

306 and NO_3^- concentrations with time are attributed to recycling of operational water
307 within the source reservoir to avoid discharge (resulting in dilution; from day 1 to
308 79) and natural variability in the source water.

309 Because the methanol addition to the injection water was calculated to provide the
310 electron donor needed to reduce the high concentrations of NO_3^- and dissolved
311 oxygen (and the much lower concentrations of Se) in the injection water, the trends
312 in concentrations of methanol (reported as DOC) added to the injection water with
313 time generally reflect that of NO_3^- (Fig. 2a and 2c). For methanol, this equated to
314 a COD:N ratio of ~ 6.5, or a DOC:N ratio of ~1.25 to 1.5 (Scheible et al, 1993). The
315 injected DOC concentration exceeded that of the source water (mean 0.75 ± 0.31
316 mg L^{-1}; n=188). The mean DOC concentration in the water injected into the SRF
317 was 31±8.2 mg L^{-1} and ranged from 0 to 103 mg L^{-1} (n=183). Upsets in the
318 methanol-dosing system resulted in several 1-d over-additions of DOC (Fig. 2c).

319 The injected Br^- tracer concentrations were generally constant with time after day
320 6 (Fig. 2d), with a mean concentration of 33±6.3 mg L^{-1} (n=183).

321 The concentrations of dissolved Se, NO_3^-, DOC, and Br^- in the water injected for
322 treatment were much greater than the background concentrations in the SRF. The
323 mean background concentrations of dissolved Se, NO_3^-, DOC, and Br^- in the
324 monitoring wells were 16±0.23 µg L^{-1} (n=70) and 0.12±0.20 (n=44), 2.55±4.07
325 (n=73), and 0.25±0.02 (n=44) mg L^{-1}, respectively. In the case of Se, the mean
326 background concentrations varied between monitoring wells, with values of

3.3±1.6 (n=14), 0.52±0.26 (n=13), 59±17 (n=13), 5.1±4.8 (n=14), and 14±3.4 (n=16) μg L^{-1} for wells 01A, 02A, 03A, 06A, and 07A, respectively.

3.1.2 Water Chemistry in the SRF

The pH values measured in the monitoring wells during the experiment were circumneutral with a mean pH of 6.81±0.31 (range 6.26 to 7.30). The DO and ORP measured in the monitoring wells reflect suboxic to mildly suboxic conditions. The mean DO concentration was 0.18±0.1 mg L^{-1} (range 0.008 to 5.25 mg L^{-1}) and the mean ORP was +70±60 mV (range −96 to +252 mV).

The Br^- concentrations in the monitoring wells increased from background values at the onset of the experiment to near injected concentrations between 41 and 68 d, depending on the well (Fig. 2d). Reactive parameters Se (Fig. 2a), NO_3^- (Fig. 2b) and DOC (Fig. 2c) initially followed a similar trend to that of the Br^- tracer (Fig. 2d) reflecting the arrival of injected water followed shortly thereafter by a decreasing trend indicative of removal.

The concentrations of dissolved Se in the monitoring wells initially followed a similar overall trend to the injected water but were considerably lower (Fig. 2a). Specifically, the concentrations increased rapidly from between 0.27 and 10 μg L^{-1} on day 1 to between 42 and 140 μg L^{-1} between day 11 and 34 (depending on the well) as injected water arrived at each respective well, then decreased due to bioreduction to between 4 and 36 μg L^{-1} between day 43 to 65. Another spike was observed with concentrations rising to between 67 and 81 μg L^{-1} between day 64 and 79, before finally decreasing sharply to <6.0 μg L^{-1} after day 117.

As was the case for Se, the NO_3^- and DOC concentrations in the monitoring wells followed similar trends to the injected water but were also significantly lower (Fig. 2b and 2c). The NO_3^- concentrations increased rapidly reflecting arrival of injected water to peak concentrations of 14.9 to 19.6 mg N L^{-1} between day 60 and 80 (depending on the well) then decreased to <0.8 mg N L^{-1} between day 110 and 120 in response to strong bioreduction. Subsequently, the concentrations typically increased slightly to maximum concentrations of 9.9 mg N L^{-1} and then decreased to <1.5 mg N L^{-1}.

Normalized Br^- concentrations (C/C_0 values) in the monitoring wells were calculated using the Br^- concentrations measured in the monitoring wells and the mean injected Br^- concentration (C_0; 33 mg L^{-1}) to estimate the amount of injected water at each well with time. The Br^- C/C_0 plots (Fig. 3a) show complete breakthrough of injected Br^- for wells 01A, 02A, 03A, 06A, and 07A on day 68, 48, 49, 62, and 57, respectively. These C/C_0 values show the post-breakthrough monitoring well waters are dominated by injection water; the mean C/C_0 values of Br^- for wells 01A, 02A, 03A, 06A, and 07A were 0.88±0.07, 0.95±0.04, 0.81±0.06, 0.93±0.05, and 0.89±0.07, respectively (Hendry et al., 2023). Using the Br^- C/C_0 plot data, Hendry et al. (2023) estimate residence times for water to travel from the injection wells to monitoring wells 01A, 02A, 03A, 06A, and 07A of 27, 9, 4, 16, and 15 d, respectively.

The normalized dissolved Se and NO_3^- concentrations for the monitoring wells were calculated in two ways: corrected and not corrected for background concentration (*C).* Unlike the Br^- concentrations that were controlled by tracer

addition, the injected Se and NO_3^- concentrations varied significantly with time, so the C_0 associated with each C (defined as C_0') was determined using residence time (*i.e.,* time lag) (Fig. 3b and 3c). The difference in the C/C_0' vs. time plots for dissolved Se and NO_3^- based on corrected and non-corrected background concentrations were negligible for wells 01A (Fig. S1a), 02A, 06A, and 07A; well 03A (Fig. S1b), however, showed a slight difference for dissolved Se because of variable pre-test Se in this well (Fig. S1). For this reason, the C/C_0' values for Se and NO_3^- (Fig. 3b and 3c) were not corrected for background concentrations.

To explain observed trends with respect to hydraulic and microbial stages, the trends in C/C_0' for Se and NO_3^- and C/C_0 for Br^- with time for individual wells were divided into three zones (Fig. 3). In Zone 1, from day 1 to between days 33 and 77, the C/C_0' for Se and NO_3^- gradually increased with time and peaked between 1.0 and 1.3. Over the same time, the C/C_0 for Br^- increased to between 0.9 and 1.0. The similarity between these C/C_0' and C/C_0 values is attributed to the breakthrough of the injected water at each well with no detectable Se or NO_3^- reduction. In Zone 2, from the end of Zone 1 to between day 117 and 132, the Se and NO_3^- C/C_0' values gradually decreased to <0.02 and <0.002 reflecting the initiation of bioreduction. In Zone 3, from the end of Zone 2 to day 201, slight increases in the Se C/C_0' (0.02 to 0.06). Greater increases in the NO_3^- C/C_0' (0 to 0.48) occurred in wells 01A, 02A, 06A, and 07A inferred to be in response to small operational shut downs and adjustments to methanol dosing. The increases in the Se and NO_3^- C/C_0' values in these wells were followed by decreases to between 0 and 0.04 and 0.01 and 0.08, respectively on day 201; these decreases were

coincident with the increased flow rate and more stable operating conditions. In contrast to these wells, the Se and NO_3^- *C/C₀'* values in well 03A did not increase in Zone 3 but remained constant and consistent with values observed in Zone 2. In summary, the time series plots of *C/C₀'* show strong Se bioreduction (<0.02) and denitrification (<0.002) occurred between day 117 and 132; *i.e.,* approximately 98% and 99.8% removal respectively.

The DOC concentrations (Fig. 2c) and *C/C₀'* (calculated as described above; Fig. 3d) support the conclusion that denitrification and Se bioreduction are occurring in the SRF. The presence of *C/C₀'* values for DOC in Zone 1 of typically <0.1 and the lack of Se and NO_3^- removal suggests the DOC is consumed close to the point of injection and used for biofilm growth and development rather than reduction. The *C/C₀'* values for DOC in wells 01A and 03A remained low in Zone 2, while the values in the three other wells increased to between 0.2 and 0.4 at the start of Zone 2. These results, coupled with the trend to complete Se bioreduction and denitrification in this zone, are in keeping with the DOC being used as the electron donor for Se bioreduction and denitrification. The increased *C/C₀'* values in some wells suggests not all added DOC was used by microbes during this stage and small adjustments to methanol dosing were made. In Zone 3, the *C/C₀'* values for DOC for all wells were mostly <0.1, with all wells decreasing to background values by the end of Zone 3 reflecting complete consumption of methanol.

3.1.3 Dissolved Se Species

Overall, the dissolved Se concentrations in the injected water and monitoring wells determined using ALS Environmental and Brooks Applied Labs methods are in

418 good agreement (Fig. 4). The good visual correlation is supported by a good best-
419 fit linear equation for the two datasets of y=0.85x+0.54b (r^2=0.98) (Fig. S2). The
420 exceptions to this well-defined trend are the dissolved Se concentrations from well
421 02A, for which the mean concentration determined by Brooks Applied Labs is
422 47±41% of the concentrations determined by ALS Environmental. Because the
423 C/C_0' values for dissolved Se for well 02A determined by ALS Environmental (i.e.,
424 1.2) are more consistent with the C/C_0 values for Br^- at end of Zone 1 (i.e., 1.1)
425 than the C/C_0' values for dissolved Se determined by Brooks Applied Labs (i.e.,
426 0.16), the dissolved Se concentrations measured by the former laboratory were
427 used in subsequent analyses.

428 The distribution of Se species with time for injected water and from monitoring wells
429 is presented in Fig. 4. The dominant aqueous Se species in the injected water was
430 Se(VI) (mean 53±25 μg L^{-1}) with Se(IV) being the second-most abundant species
431 (mean 13±2.3 μg L^{-1}), as is typical in near neutral pH surface waters (*cf*. Chan et
432 al, 2009). The concentrations of SeMe, $SeSO_3$, MeSe(IV), and SeCN in the
433 injected water were reported at the LLD; DMSeO concentrations were also at the
434 LLD in the injected water except for two time periods: when results were 0.011 μg
435 L^{-1} on day 84 and between 0.011 to 0.015 μg L^{-1} between days 140 and 159. The
436 presence of DMSeO may suggest off-gassing of volatile Se species (Wozniak and
437 Gerads, 2018).

438 In keeping with the dominance of Se(VI) and, to a lesser extent, Se(IV) in the
439 injected water, the dominant Se species in the monitoring wells in Zone 1 was
440 Se(VI) (mean 31±18 μg L^{-1}) followed by Se(IV) (mean 2.2±2.4 μg L^{-1}). The Se

441 speciation data show the removal of Se in Zone 2 (Figs. 3b and 4) was dominated
442 by marked decreases in the concentrations of Se(VI) in all wells and, in wells 03A
443 and 07A where Se(IV) concentrations were higher initially, a clear decrease in
444 Se(IV) was observed. By the end of Zone 2, the Se(VI) concentrations were
445 between 0.06 and 0.62 μg L^{-1} and Se(IV) concentrations were similar, between
446 0.11 and 0.68 μg L^{-1} (Fig. 4). The increased dissolved Se concentrations in wells
447 01A, 02A, and 07A in Zone 3 were dominated by Se(VI) (mean 0.81±0.95 μg L^{-1})
448 and to a lesser extent Se(IV) (mean 0.41±0.20 μg L^{-1}) (Fig. 4b, c, and f). At the
449 end of the field experiment, Se(VI) and Se(IV) concentrations were low in all wells.
450 Most wells had slightly higher Se(VI) than Se(IV); in well 06A, Se(IV) (mean
451 0.28±0.19 μg L^{-1}) was greater than Se(VI) (mean 0.09±0.05 μg L^{-1}) (Fig. 4e). Clear
452 and consistent temporal relationships between changes in Se(VI) and Se(IV) as
453 an intermediate reduction product such as those described in the literature (*c.f.*
454 Siddique et al., 2007) were not observed at this scale, perhaps due to the low
455 concentrations and spatial variability of the biogeochemical reduction process.

456 The concentrations of SeMe, SeCN, $SeSO_3$, and DMSeO in all monitoring well
457 waters were, with few outliers, reported at the LLD (Fig. 4). Minor concentrations
458 of MeSe(IV) (maximum concentration 0.033 ug L^{-1} at well 06A) and DMSeO
459 (maximum concentration 0.042 μg L^{-1} at well 06A) were measured in multiple
460 monitoring wells in all zones (Fig. 4). The low but measurable concentrations of
461 these Se species is speculated to reflect off-gassing of volatile Se species
462 (Wozniak and Gerads, 2018); however, the cause is not clear and may warrant
463 investigation.

464 *3.1.4 Sequestered Selenium*

465 The calculated total mass of Se injected into the full scale field experiment over
466 the 201-day period was 67 kg. The mass of Se attenuated in the system was 59
467 kg over the same period, equating to an attenuation of approximately 0.3 kg d^{-1}.
468 Based on the data presented to this point in the paper, the form of attenuated Se
469 at the field scale is not known; however, the results of the column experiments,
470 discussed below, identify the attenuation mechanism.

471 3.2 Column Experiments

472 *3.2.1 Water Chemistry*

473 The column experiments used amended SRF water as influent, with
474 concentrations of 1.0 mg L^{-1} Se(VI) as Se and 30 mg NO_3^--N L^{-1}, and negligible
475 oxygen. The trends in pH, DO, and ORP with time in the effluent from columns 9
476 and 10 were the same, suggesting good reproducibility between columns (Fig. S3).
477 The mean pH from column 9 and 10 effluents was 7.83±0.15 and 7.78±0.21 and
478 the DO and ORP in the effluents were 4.40±1.85 and 3.61±2.48 mg L^{-1} and -
479 18.5±80.7 and -37.8±91.5 mV, respectively. The pH of the column effluent samples
480 was slightly higher than the monitoring well samples in the field experiment,
481 potentially reflecting a slightly higher pCO_2 and lower pH in the field relative to the
482 lab or production of alkalinity during denitrification. Although the DO measured in
483 column effluent suggests oxygen levels were higher than in the monitoring wells,
484 the column ORP values were slightly lower, though still within the range observed
485 in the field experiment. The discrepancies between the field and column values
486 may be attributed to measurements in the effluent collection vessel, which could

not be fully isolated from the atmosphere. The differences are not considered important.

Due to the relatively short residence time in the columns (~64 h; determined using Br^- tracer tests; data not presented), the C/C_0 calculations were not adjusted for time lag. Additionally, columns had previously been operated and had an established biomass at the start of the column experiments; therefore, water chemistry presented here is most comparable to the Zone 3 time period described for the field experiment. Most of the influent Se concentration (1.0 mg L^{-1}) was reduced in columns 9 and 10, with isolated upset conditions observed due to intermittent feed line blockage (*e.g.,* days 57, 112, 301, 343, and 385 in column 9 and days 40, 68, 138, and 351 in column 10) (Fig. 5a). Overall, the mean Se concentrations in the effluent water from columns 9 and 10 were 0.08±0.13 and 0.10±0.16, which equates to a range in C/C_0 values from ~0.08 to ~0.10 (Fig. S4a).

The dissolved NO_3^- concentrations with time in effluent water samples from columns 9 and 10 exhibit similar trends to those for Se. Most of the influent NO_3^- (30 mg N L^{-1}) was reduced before exiting the column (Fig. 5b). Overall, the mean NO_3^- concentrations in the effluent waters from columns 9 and 10 were 0.52±1.03 and 0.53±1.27 mg N L^{-1}, which equate to C/C_0 values of ~0.02 (Fig. S4b).

The trends in DOC in the column effluent (Fig. 5c) show most of the influent DOC was consumed, reducing concentrations to 1.83 and 1.50 mg L^{-1} by day 63 (C/C_0 of ~0.02; Fig S4c). This suggests biofilm growth in conjunction with Se and NO_3^- removal in columns 9 and 10, respectively. While this level of detailed data could

not be collected for column 12, the limited data available for column 12 show it performed comparably. The DOC concentrations in the effluent from both columns 9 and 10 increased to ~57 mg L^{-1} (C/C_0 of 0.75; Fig S4c) at day 126, then gradually decreased with time to 7.11 and 5.06 mg L^{-1} (C/C_0 of ~0.08; Fig S4c) on day 462. This was followed by more efficient use of DOC by the biofilm.

The trends observed in the column effluent samples for dissolved Se, NO_3^-, and DOC concentrations demonstrated microbial reduction of Se and NO_3^- with associated removal of DOC. The dissolved Se and NO_3^- concentrations in the column effluent are also consistent with data from the field experiment Zone 3.

3.2.2 Dissolved Se Species

The consistent distribution of Se species in the effluent of columns 9 and 10 is presented in Fig. S5. In the column effluent, the Se(VI) remained the dominant dissolved Se species (mean 137±307 µg L^{-1}) and constituted, on average, 48% of the remaining dissolved Se. These effluent Se(VI) concentrations were 85.1% lower than the Se(VI) concentration in the influent (1.0 mg L^{-1}). Se(IV) was the second-most abundant Se species in the column effluent (mean 47.5±96.9 µg L^{-1}) and constituted, on average, 34% of the dissolved Se. This reflects the partial reduction of Se(VI) to the intermediate species Se(IV), which was either sorbed or further reduced to Se(0). Due to intermittent changes in flow and nutrient supply during column testing, the relative ratio of Se(VI) to Se(IV) varied such that the temporal relationships of Se(VI) reduction to Se(IV) reported by Siddique et al. (2007) were not observed here. Further, SeCN, MeSe(IV), $SeSO_3$, unknown species, DMSeO, and SeMe were present in lesser, but measurable,

concentrations in the effluent of 1.33±0.88, 1.27±1.28, 0.49±0.61, 0.30±0.26, 0.11±0.28, and 0.01±0.02 μg L^{-1} that represent 7.3, 6.4, 2.0, 1.9, 0.2, and 0.04% of the dissolved Se, respectively. These concentrations were greater than those observed at the field scale as might be expected when one is able to monitor much closer to the active microbial community.

3.2.3 Microbiology

The microbial community of the baseline waste rock sample was diverse and comprised of bacteria reported to have the capacity for Se reduction (*e.g., Rhizobium selenitireducens* (Hunter et al., 2007), *Geobacter* sp. (Pearce, et. al., 2009), and *Rhodoferax* sp., (Kirk, 2014), denitrification (*e.g., Pseudomonas* sp.), iron (Fe) oxidation and reduction (*e.g., Ferribacterium* sp., *Geobacter* sp., and *Rhodoferax* sp.), sulfur oxidation and reduction (*e.g., Desulfobacterium* sp., *Desulfovibrio* sp.), and hydrocarbon degradation (*e.g., Pseudomonas* sp.). The top 20 identified taxa (of 404 taxa identified by sequencing) for samples collected post-testing from 0, 0.1, and 0.3 m from columns 9 and 10 are summarized in Fig. 6. The relative abundance of Proteobacteria, including *Thiobacillus sp., Rhodoferax sp., Methylotenera sp., Hydrogenophilaceae*, and *Ferribacterium sp.*, and Bacteroidota (such as *Bacteroidetes*) declined with distance from the point of methanol injection, while the abundance of Firmicutes (*e.g., Desulforsporosinus* sp.) and Desulfobacterota (*e.g., Geobacter* sp.) increased. These genera are grouped by putative function in Fig. S6. The relative abundance of nitrate-reducing organisms (such as *Thiobacillus* (Baldensperger and Garcia, 1975) and *Methylotenera* (Kalyuhznaya et al., 2009)) shifted from 22.5 to 13.5% between the influent and

555 effluent portion of the columns. Nitrite-reducing organisms shifted from 12 to less
556 than 6% over this distance, while the abundance of Se- and Fe-reducers increased
557 in relative abundance from 5 and 6% to 9 and 10%, respectively, with their
558 maximum abundance occurring mid-column (Fig. S7). The identified Se-reducing
559 organisms included several species from the genera *Desulfovibrio* (Tomei et al.,
560 1995), *Geobacter* (Pearce et al., 2009), *Dechloromonas* (Kirk, 2014), and
561 *Pseudomonas* (Ike et al., 2000). The relative abundance of methanol-consuming
562 organisms declined from influent to effluent zones, offset by increases in
563 organisms capable of sulfate (SO_4^{2-}) reduction and chemoheterotrophy at the
564 effluent portion of the column (Fig. S7).

565 At the influent end of the columns, organisms with the capacity for NO_3^-/NO_2^-
566 reduction and methanol oxidation were most abundant; the mid-column (0.1 m)
567 samples showed increased capacity for Se and Fe reduction; and effluent samples
568 (where oxygen is likely lower) reflected an increase in SO_4^{2-} reducers.

569 The native microbial communities present in the SRF during operation also
570 exhibited the potential for methanol oxidation, denitrification, and Se reduction,
571 and the relative abundance of microorganisms capable of these functions was
572 greater within the active treatment zone compared to distal areas of the
573 SRF (data not presented).

574 *3.2.4 Sequestered Selenium*

575 The calculated total masses of Se sequestered in columns 9, 10, and 12 during
576 the experiment (*i.e.*, the difference between the mass introduced into the column

577 and that recovered in the effluent) were 79.9, 62.8, and 72.8 mg kg^{-1} waste rock.
578 This concentration is much greater than the total Se concentrations measured in
579 the three subsamples from column 12 (18.5, 18.8, and 19.3 mg kg^{-1} at 0.0, 0.1,
580 and 0.3 m from the inlet, respectively). The calculated total mass of Se
581 sequestered in the columns and the measured concentrations in the columns are
582 both much greater than the total Se concentration in the pre-test sample (1.73 mg
583 kg^{-1}). These results support the conclusion that Se is sequestered in the column;
584 however, the total Se concentrations measured in the subsamples collected along
585 the column only represent ~25% of the calculated mass of Se sequestered in the
586 column. The reason for the difference between the total Se concentrations
587 measured in the three column samples and the total mass of Se sequestered in
588 the column during the experiment is not clear and may be attributed to in-column
589 variations and/or sampling biases such as sampling the full grain size distribution
590 or excluding localized biomass and biomineralization that could result from
591 preferential flow. Some fraction of the Se may also have been volatilized as H_2Se
592 gas, which was not measured. The XANES Se spectra of column 12 samples
593 suggest Se in the sample is predominantly (~94%) as Se(0) in Se-S ring
594 compounds represented by the formula Se_nS_{8-n} (Table S1) (Laitenen, 1987) and
595 Se(0), which is considered insoluble in natural environments (Minaev et al., 2005).
596 The XANES spectrum suggest the remainder of Se in the sample is present as
597 Se(IV). If the Se is present as mixed Se-S compounds, the analysis suggests the
598 Se:S molar ratio aligns with Se_2S_6. Additional details on fitting of the XANES
599 spectra are presented in Figs. S8 and S9.

3.3 Selenium Bioreduction

Se bioreduction can reduce selenate (Se(VI)) to selenite (Se(IV)) and then to insoluble elemental Se (Se(0)) (*cf.,* Minaev et al., 2005; Buchs et al., 2013, Boltz and Rittmann, 2021). The overall process of the microbial reduction of Se(VI) (as SeO_4) leading to the formation of relatively insoluble Se^0 (Debieux et al., 2011) can be represented by equations (1) and (2):

$$SeO_4^{2-} + 2e^- + 2H^+ \rightarrow SeO_3^{2-} + H_2O \quad [1]$$

$$SeO_3^{2-} + 4e^- + 6H^+ \rightarrow Se^0 + 3H_2O \quad [2]$$

Multiple lines of evidence from the field and column experiments support Se attenuation via Se bioreduction by indigenous bacteria as described in equations [1] and [2]. These lines of evidence include: the near complete removal of Se(VI) and Se(IV) in the SRF injection water by the end of Zone 2 at the field scale and in the column effluent; the consumption of the labile organic carbon (methanol) required for the bioreduction of NO_3^- and Se in both the field and column experiments; the presence of indigenous Se-reducing organisms in the columns and in the field; the dominance of Se-S compounds (*i.e.,* S(0)) in the Se sequestered in the column experiments; and Se(VI) being the dominant Se species in the SRF and column effluent followed by Se(IV). The observation that the sequestered Se is in the form of Se(0) is consistent with investigations which show anaerobic and facultative bacteria can form Se(0) particles (Vogel et al., 2018; Bajaj et al., 2012) by reducing Se oxyanions. Vogel et al. (2018) further show bacteria can reduce Se(IV) to extracellular Se_nS_{8-n} structured particles. The Se

622 bioreduction process is further supported by a Pourbaix diagram (Fig. S10) that
623 shows Se stability fields shifting from Se(IV) in the SRF injection water to Se(0) in
624 the monitoring wells.

625 Evidence of the *in situ* Se bioreduction of dissolved Se(VI) and Se(IV) to Se(0) by
626 indigenous bacteria is consistent with several other studies from the Elk Valley.
627 Deen et al. (2018) show Se bioreduction can occur in waste rock in the Elk Valley
628 under anoxic, water-saturated laboratory conditions using the labile organic carbon
629 available in the coal-rich waste rock. Martin et al. (2011) show the sequestration of
630 Se as Se(0) and Se(-II) in marsh and the oxbow sediments in the Elk Valley while
631 the overlying water columns contained Se(VI). The bioreduction of Se(VI) to Se(0)
632 in a laboratory-based study of coal mine tailings pond sediments is reported by
633 Siddique et al. (2007). Bioreduction of Se(VI) to insoluble Se species has also been
634 reported in a mine pit backfilled with water-saturated waste rock (Bianchin et al.,
635 2013; Kirk, 2014) and in unsaturated coarse coal reject piles (Kennedy et al.,
636 2015).

637 The overall lack of measurable concentrations of SeMe, $SeSO_3$, SeCN, MeSe(IV),
638 and DMSeO in the monitoring well waters in the field experiment is also consistent
639 with equations [1] and [2]. In contrast to the SRF results, measurable but low
640 concentrations of SeCN, MeSe(IV), $SeSO_3$, unknown species, DMSeO, and SeMe
641 were measured in column effluent samples. Little is known regarding the
642 biogeochemistry of these compounds and their formation, though Wozniak and
643 Gerads (2018) provide some context to suggest that when these compounds are
644 observed in bioreactor effluents, they may indicate cell death (SeCN), sulphate

reduction ($SeSO_3$), de-gassing of volatile species or shifts in the microbial community. It would be expected therefore that samples from the column experiments collected near an active microbial community would be more likely to contain these compounds than samples collected at the field scale (*i.e.,* at greater distances from the active biomass or where potential exists for dilution). The differences could also reflect the bioreduction of a much greater concentration of Se(VI) in the columns compared to the field experiment (*i.e.,* 1.0 mg L^{-1} vs. 88 µg L^{-1}). At present, however, we cannot definitively explain the presence of these secondary Se species in the column effluent but not in the field experiment. Further study of this difference may be warranted.

3.4 Inhibition of Se(VI) Reduction

Several factors can inhibit Se(VI) bioreduction in the presence of NO_3^-. While NO_3^- and Se(VI) can be reduced concurrently (Oremland et al., 1999), Oremland reported NO_3^- inhibition of Se(VI) reduction in (Oremland et al., 1989) and NO_2^- inhibition in (Oremland et al., 1994). Given the much greater concentrations of NO_3^- than Se(VI) in influent, and the fact that Se(VI) can be reduced by NO_3^-reductase enzymes (Sabaty et al, 2001), and Se(IV) can be reduced by NO_2^-reductase enzymes (De-Moll-Decker and Macy, 1993) on a non-specific basis, this inhibition may in part, reflect competition between NO_3^- / NO_2^- and Se(VI)/Se(IV), respectively, for the enzyme substrates. It may also reflect the relative abundance and overall genetic capacity of Se(VI) and NO_3^- reducing microorganisms in the biofilm. Recent work by Kulasekara et al. (2023) show greater inhibition of Se(IV) reduction than Se(VI) by NO_3^- , with an associated shift

668 in microbial community (and elevated NO_3^- concentrations inhibit Se(VI) reduction)
669 (*cf.,* Bailey et al., 2012; Gates et al., 2009). In the case of the latter, Bailey et al.
670 (2012) show inhibition occurs when NO_3^- concentrations exceed 1 mg N L^{-1} while
671 Gates et al. (2009) suggest inhibition occurs at NO_3^- concentrations >2.3 mg N L^{-1}.
672 The extensive suites of Se and NO_3^- concentration data from the field experiment
673 and the columns allowed us to assess the inhibition of Se(VI) reduction by NO_3^- at
674 both scales. To test inhibition in the field experiment, we calculated the percent Se
675 reduction (Se_p) and percent NO_3^- denitrified (NO_{3p}) in Zones 2 and 3 (no
676 measurable Se bioreduction or denitrification occurred in Zone 1). The Se_p and
677 NO_{3p} for each monitoring well with time were calculated by subtracting the dilution-
678 corrected C/C_0' values (*i.e.,* dividing the C/C_0' by the mean C/C_0 values for Br^- of
679 0.88, 0.95, 0.81, 0.93, and 0.89 for wells 01A, 02A, 03A, 06A, and 07A,
680 respectively) from the mean C/C_0 Br^- values for each monitoring well, then dividing
681 by the mean C/C_0 Br^- values for each well.

682 The Se_p values exhibited similar well-defined trends over time for all wells (Fig. 7).
683 The Se_p values increased from −16 to 8.7% at the start of Zone 2 to >99% between
684 day 117 and 134. The Se_p values in wells 01A, 02A, 06A, and 07A decreased
685 slightly (93 and 98%) between day 177 and 184. In addition, the Se_p values in well
686 02A exhibited a spike to 79% on day 64.

687 The evolution of NO_{3p} also exhibited well-defined trends over time for all wells,
688 consistent with the overall evolution of the Se_p values (Fig. 7). NO_{3p} increased from
689 zero (or negative) at the start of Zone 2 to 100% between day 114 and 141.
690 Consistent with the Se_p values, the NO_{3p} in wells 01A, 02A, 06A, and 07A

691 decreased to between 50 and 90% between day 130 and 197, before increasing
692 to between 90 and 100% by the end of the experiment. Also consistent with the
693 Se_p values, the NO_{3p} values for well 03A (Fig. 7c) did not decrease between day
694 130 and 197.

695 The good agreement between NO_{3p} and Se_p values with time in the wells in Fig. 7
696 is supported by the good (r^2=0.79) best-fit linear regression to the cross-plotted
697 NO_{3p} and Se_p values from Zones 2 and 3 for the monitoring wells (Fig. S11). The
698 SRF observations show that, under the range in NO_3^- and Se concentrations
699 tested and at the scale of measurement (*i.e.,* the closest monitoring wells to the
700 injection wells were ~35 m), both species were removed from the injected water
701 concurrently. In the case of the column tests, the very low concentrations of both
702 Se and NO_3^- in the effluent suggest the length of the reduction zone is less than
703 the length of the columns; in other words, the hydraulic residence time exceeds
704 the time required for reduction. These observations are consistent with laboratory
705 and field studies by others that show simultaneous reduction of NO_3^- and Se(VI)
706 at the scales tested (*cf.*, Bianchin et al., 2013; Macy et al., 1993; Oremland et al.,
707 1999, Sabaty et al., 2001). These data, including ours, are however not consistent
708 with other studies that demonstrate elevated NO_3^- concentrations inhibit Se(VI)
709 reduction (*c.f.,* Bailey et al., 2012; Gates et al., 2009). This is perhaps due to biofilm
710 heterogeneity and different biological mechanisms for Se reduction that rely on
711 different enzymes (*i.e.*, NO_3^-reductase vs. Se(VI) reductase), each with specific
712 enzyme kinetics and potential inhibitors. This is especially true in a mixed

community of native biofilm organisms with overlapping capacity to reduce nitrate and/or selenate.

Our data do not, however, preclude the inhibition of Se(VI) reduction by NO_3^- in the field or in the column experiments closer to the points of injection. All NO_3^- may be reduced closer to the points of injection and the Se(VI) bioreduced slightly downgradient of the denitrification zone but before the end of the columns or the first row of monitoring wells. This is supported by the observation of a shift from denitrifying to Se(VI)-reducing organisms from the influent to midpoint of the columns and supported by *in situ* SRF microbial community data from biocoupons (data not presented) that demonstrate a shift from denitrifiers to Se-reducing organisms with distance from the injection point.

4. CONCLUSIONS

Building on the well-established knowledge base on the bioreduction of Se(VI) and NO_3^- in suboxic environments, a long-term (201 d), *in situ* bioremediation field experiment successfully treated a large volume (up to 7500 m^3 d^{-1}; total 931,000 m^3) of Se(VI)- and NO_3^--contaminated water (mean 88 µg Se L^{-1} and 22 mg N L^{-1}) to <3.0 µg Se L^{-1} and <0.5 mg N L^{-1}. Following completion of this field experiment, the SRF has continued to bioremediate Se(VI)- and NO_3^--contaminated wastewater as described above. As of February 1, 2023 (day 1,847), 17 Mm^3 of wastewater with 1,600 and 275,000 kg of Se and NO_3^- has been treated in this SRF. Complementary long-term column experiments confirmed bioreduction of Se(VI) and NO_3^- in the presence of Se- and NO_3^--reducing bacteria on column

735 solids, and reduced Se mostly in the form of inert Se(0), likely in Se-S ring
736 compounds.

737 At the scales tested, field and column data show that NO_3^- and Se are effectively
738 reduced concurrently with no observed inhibition of Se reduction by NO_3^-.

739

740 ***CRediT authorship contribution statement***

741 M. Jim Hendry: Conceptualization, Methodology, Writing – original draft, Writing –
742 review & editing. Lisa Kirk: Methodology, Data curation, Writing – review & editing.
743 Jeff Warner: Methodology, Data curation, Writing – review & editing. Shannon
744 Shaw: Writing – review & editing. Brent M. Peyton: Writing – review & editing.
745 Schmeling: Methodology, Writing – review & editing, Data curation. S. Lee
746 Barbour: Writing – review & editing.

747 ***Data availability***

748 The data that have been used are confidential.

749 ***Declaration of competing interest***

750 The authors declare the following financial interests/personal relationships which
751 may be considered as potential competing interests: Jim Hendry reports a
752 relationship with Teck Resources Limited that includes: consulting or advisory. Lisa
753 Kirk reports a relationship with Teck Resources Limited that includes: consulting
754 or advisory. Jeff Warner reports a relationship with Teck Resources Limited that
755 includes: consulting or advisory. Shannon Shaw reports a relationship with Teck
756 Resources Limited that includes: consulting or advisory. Brent Peyton reports a
757 relationship with Teck Resources Limited that includes: consulting or advisory. Erin

Schmeling reports a relationship with Teck Resources Limited that includes: consulting or advisory. Lee Barbour reports a relationship with Teck Resources Limited that includes: consulting or advisory.

Acknowledgements: Financial support to undertake this study was provided by Teck Resources Ltd. The manuscript benefited from discussions with members of the external technical oversight advisory panel of experts for this experiment. Enviromin Inc. team members including Katharine Seipel, Rachel Spietz, Ethan Wologo, and Seth D'Imperio supported this work.

References

ATSDR (Agency for Toxic Substances and Disease Registry), 2003. Toxicological profile for selenium. Agency for Toxic Substances and Disease Registry, Public Health Service, U.S. Department of Health and Human Services, Atlanta, Georgia. http://www.atsdr.cdc.gov/toxprofiles/tp92.pdf

Aqueous Solutions, LLC, 2023. The Geochemist's Workbench 2023, Release 17.0.0.

Bailey, R.T., Hunter, W.J., Gates, T.K., 2012. The influence of nitrate on selenium in irrigated agricultural groundwater systems. *Journal of Environmental Quality,* 41(3), 783-92.

Baldensperger, J., Garcia, J. L., 1975. Reduction of oxidized inorganic nitrogen compounds by a new strain of *Thiobacillus denitrificans*. *Archives of Microbiology*, 103(1):31-36.

Bajaj, M., Schmidt, S., Winter, J., 2012. Formation of Se(0) nanoparticles by

Duganella sp. and *Agrobacterium sp*. isolated from Se-laden soil of North-East Punjab, India. *Microbial Cell Factories*, 11, 1-14.

Beatty, J. M., Russo, G. A., 2014. Ambient water quality guidelines for selenium. A Technical Report Update. BC Ministry of Environment. 270p.

Bianchin, M., Martin, A. J., Adams, J., 2013. In-situ immobilization of selenium within the saturated zones of backfilled pits at coal-mine operations. British Columbia Mine Reclamation Symposium.

Boltz, J. P., Rittmann, B. E., 2021. Microbial ecology of selenium-respiring bacteria. *Environmental Technologies to Treat Selenium Pollution: Principles and Engineering* . IWA Publishing, 145-170.

British Columbia Ministry of Environment and Climate Change Strategy., 2023. British Columbia approved water quality guidelines: aquatic life, wildlife & agriculture - guideline summary. *Water Quality Guideline Series*, WQG-20. Prov. B.C., Victoria B.C., 42 pp.

Buchs, B., Evangelou, M. W., Winkel, L. H., Lenz, M., 2013. Colloidal properties of nanoparticular biogenic selenium govern environmental fate and bioremediation effectiveness. *Environmental Science & Technology*, 47(5), 2401-2407.

Callahan, B. J., McMurdie, P. J., Rosen, M. J., Han, A. W., Johnson, A. J., Holmes, S. P., 2016. DADA2: High resolution sample inference from Illumina amplicon data. *Nature Methods,* 13(7), 581-583.

Chan, Y.T., Kuan, W.H., Chen, T.Y., Wang, M.K., 2009. Adsorption mechanism of selenate and selenite on the binary oxide systems. *Water Res.* 43, 4412–4420.

Comeau, A. M., Li, W. K., Tremblay, J. É., Carmack, E. C., Lovejoy, C., 2011.

Arctic Ocean microbial community structure before and after the 2007 record sea ice minimum. *PloS One*, 6(11), e27492.

Debieux, C. M., Dridge, E. J., Mueller, C. M., Splatt, P., Paszkiewicz, K., Knight, I., Florance, H., Love, J., Titball, R.W., Lewis, R.J., Richardson, J., Butler, C. S., 2011. A bacterial process for selenium nanosphere assembly. *Proceedings of the National Academy of Sciences*, 108(33), 13480-13485.Deen, S. G., Bondici, V. F., Essilfie-Dughan, J., Hendry, M. J., Barbour, S. L., 2018. Biotic and abiotic sequestration of selenium in anoxic coal waste rock. *Mine Water and the Environment*, 37, 825-838.

DeMoll-Decker, H., Macy, J.M. 1993. The periplasmic nitrite reductase of Thauera selenatis may catalyze the reduction of selenite to elemental selenium. Arch. Microbiol. 160, 241–247.

Dessouki, T., Ryan, A., 2010. Canada-British Columbia Water Quality Monitoring Agreement: Water Quality Assessment of the Kootenay, Elk, and Mary Rivers. BC Ministry of Environment and Environment Canada, pp. 1-55.

Frankenberger, W.T., Engberg, R.A., 1998. Environmental chemistry of selenium. Taylor & Francis Group, L.L.C., 714 pp.

Gates, T. K., Cody, B. M., Donnelly, J. P., Herting, A. W., Bailey, R. T., Mueller Price, J., 2009. Assessing selenium contamination in the irrigated stream–aquifer system of the Arkansas River, Colorado. *Journal of Environmental Quality*, 38(6), 2344-2356.

Griffith, M. B., Norton, S. B., Alexander, L. C., Pollard, A. I., LeDuc, S. D., 2012. The effects of mountaintop mines and valley fills on the physicochemical quality of

828 stream ecosystems in the central Appalachians: a review. *Science of the Total*
829 *Environment*, 417, 1-12.
830 Health Canada, 2014. Guidelines for Canadian Drinking Water Quality: Guideline
831 Technical Document – Selenium. 2014-03. https://www.canada.ca/en/health-
832 canada/services/publications/healthy-living/guidelines-canadian-drinking-water-
833 quality-guideline-technical-document-selenium.html
834 Hendry, M. J., Biswas, A., Essilfie-Dughan, J., Chen, N., Day, S. J., Barbour, S. L.,
835 2015. Reservoirs of selenium in coal waste rock: Elk Valley, British Columbia,
836 Canada. *Environmental Science & Technology*, 49(13), 8228-8236.
837 Hendry, M. J., Barbour, S. L., Schmeling, E. E., Wassenaar, L. I., Shaw, S.,
838 Schabert, M. S., 2023. Quantifying denitrification in a field-scale bioremediation
839 experiment. *Science of the Total Environment*, 854, 158762.
840 Hunter, W.J., Kuykendell, L. D., Manter, D. K., 2007. *Rhizobium selenireducens*
841 sp. nov.: A Selenite-Reducing alpha-*Proteobacteria* Isolated from a Bioreactor.
842 *Current Microbiology*, 55, 455-460.
843 Ike, M., Takashi, K., Fujita, T., Kashiwa, M., Fujita, M., 2000. Selenate reduction
844 by bacteria isolated from aquatic environment free from selenium contamination.
845 *Water Research*, 34(11), 3019-3025.
846 Kalyuhznaya, M. G., Martens-Habbena, W., Wang, T., Hackett, M. Stolyar, S. M.,
847 Stahl, D. A., Lidstrom, M. E., Christoserdova, L., 2009. *Methyloohilaceae* link
848 methanol oxidation to denitrification in freshwater lake sediment as suggested by
849 stable isotope probing and pure culture analysis. *Environmental Microbiology*
850 *Reports*, 1(5), 385-392.

851 Kalasekara, H.M.I.P, Zhang, Y., and Papelis, C. 2023. Effect of Nitrate Presence
852 on Selenium Bioremediation in Chemically Modified Zeolite Columns. Water 15,
853 1841.
854 Kennedy, C., Day, S., Mackie, D., Pesonen, N., 2015. Biogeochemical selenium
855 sequestration in unsaturated coal reject piles. *Proceedings, 10th International*
856 *Conference on Acid Rock Drainage,* 107-117.
857 Kennedy, C. J., McDonald, L. E., Loveridge, R., Strosher, M. M., 2000. The effect
858 of bioaccumulated selenium on mortalities and deformities in the eggs, larvae, and
859 fry of a wild population of cutthroat trout (Oncorhynchus clarki lewisi). *Archives of*
860 *Environmental Contamination and Toxicology*, 39, 46-52.
861 Kirk, L. M. B., 2014. *In situ* microbial reduction of selenate in backfilled phosphate
862 mine waste, SE Idaho. PhD thesis, Montana State University.
863 https://api.semanticscholar.org/CorpusID:91869131
864 Lai, C. Y., Song, Y., Wu, M., Lu, X., Wang, Y., Yuan, Z., Guo, J., 2020. Microbial
865 selenate reduction in membrane biofilm reactors using ethane and propane as
866 electron donors. *Water Research*, 183, 116008.
867 Laitinen, R. S., 1987. Selenium sulfide ring molecules. *Acta Chemica*
868 *Scandinavica*, 41, 361-376.
869 Lemly, A. D., 1993. Guidelines for evaluating selenium data from aquatic
870 monitoring and assessment studies. *Environmental Monitoring and*
871 *Assessment*, 28, 83-100.
872 Lenz, M., Len, P.N.L., 2009. The essential toxin: The changing perception of
873 selenium in environmental sciences. *Science of the Total Environment*, 407 (12),

874 3620-3633.
875 Lindberg, T. T., Bernhardt, E. S., Bier, R., Helton, A. M., Merola, R. B., Vengosh,
876 A., Di Giulio, R. T., 2011. Cumulative impacts of mountaintop mining on an
877 Appalachian watershed. *Proceedings of the National Academy of*
878 *Sciences*, 108(52), 20929-20934.
879 Louca, S., Parfrey, L. W., Doebeli, M., 2016. Decoupling function and taxonomy in
880 the global ocean microbiome. *Science*, 353(6305), 1272-1277.
881 Macy, J. M., Lawson, S., DeMoll-Decker, H., 1993. Bioremediation of selenium
882 oxyanions in San Joaquin drainage water using *Thauera selenatis* in a biological
883 reactor system. *Applied Microbiology and Biotechnology*, 40, 588-594.
884 Martin, A. J., Simpson, S., Fawcett, S., Wiramanaden, C. I., Pickering, I. J., Belzile,
885 N., Chen, Y.W., London, J., Wallschläger, D., 2011. Biogeochemical mechanisms
886 of selenium exchange between water and sediments in two contrasting lentic
887 environments. *Environmental Science & Technology*, 45(7), 2605-2612.
888 Martin, M., 2011. Cutadapt removes adapter sequences from high-throughput
889 sequencing reads. *EMBnet Journal*, 17(1), 10-12.
890 McDonald, L.E., Strosher, M.M., 1998. Selenium mobilization from surface coal
891 mining in the Elk River Basin, British Columbia: a survey of water, sediment and
892 biota. The Technical and Research Committee on Reclamation, Cranbrook, BC,
893 Canada.
894 Minaev, V. S., Timoshenkov, S. P., Kalugin, V. V., 2005. Structural and phase
895 transformations in condensed selenium. *Journal of Optoelectronics and Advanced*
896 *Materials*, 7(4), 1717.

897 Nanchariah, Y.V., Lens, P. N., 2015. Ecology and biotechnology of selenium-
898 respiring bacteria. *Microbiology and Molecular Biology Reviews*, 79(1), 61-80.
899 Oremland, R.S., Hollibaugh, J.T., Maest, A.S., Presser, T.S., Miller, L.G. and
900 Culbertson, C.W., 1989. Selenate Reduction to Elemental Selenium by Anaerobic
901 Bacteria in Sediments and Culture: Biogeochemical Significance of a Novel,
902 Sulfate-Independent Respiration. Applied and Env Microbiology, 55(9), 2333-
903 2343,
904 Oremland, R.S., Blum, J.S. Culbertson, C.W., Visscher, P.T., Miller, L.G., Dowdle,
905 P., and Strohmaier, F.E., 1994. Isolation, Growth and Metabolism of an Obligately
906 Anaerobic, Selenate-Respiring Bacterium, Strain SES-3. Appl Env Micro 60(8),
907 3011-3019.
908 Oremland, R. S., Blum, J. S., Bindi, A. B., Dowdle, P. R., Herbel, M., Stolz, J. F.,
909 1999. Simultaneous reduction of nitrate and selenate by cell suspensions of
910 selenium-respiring bacteria. *Applied and Environmental Microbiology*, 65(10),
911 4385-4392.
912 Pearce, C. I. Pattrick, R. A. D., Law, N., Charnock, J. M., Coker, V. S., Fellowes,
913 J. W., Oremland, R. S., Lloyd, J. R., 2009. Investigating different mechanisms for
914 biogenic selenite transformations: *Geobacter sulfurreducens, Shewanella*
915 *oneidensis,* and *Veillonella atypica*. *Environmental Technology*, 30(12), 1313-
916 1326.
917 Ravel, B., Newville, M., 2005. ATHENA, ARTEMIS, HEPHAESTUS: data analysis
918 for X-ray absorption spectroscopy using IFEFFIT. *Journal of Synchrotron*
919 *Radiation,* 12, 537-541.

Sabaty, M., Avazeri, C., Pignol, D., Vermeglio, A., 2001. Characterization of the Reduction of Selenate and Tellurite by Nitrate Reductases. *Applied and Environmental Microbiology*, 67(11), 5122-5126.

Siddique, T., Arocena, J.M., Thring, R.W., Zhang, Y, 2007. Bacterial reduction of selenium in coal mine tailings pond sediment. *Journal of Environmental Quality*, 36, 621-627.

Storb, M.B., Bussell, A.M., Caldwell Eldridge, S.L., Hirsch, R.M., Schmidt, T.S., 2023, Growth of Coal Mining Operations in the Elk River Valley (Canada) Linked to Increasing Solute Transport of Se, NO_3^-, and SO_4^{2-} into the Transboundary Koocanusa Reservoir (USA−Canada). *Environmental Science & Technology*, 57(45), 17465-17480.

Swanson, S., 2010. The way forward: a strategic plan for the management of selenium at Teck Coal operations. The strategic advisory panel on selenium management. Report prepared for Teck Coal Ltd, Calgary, AB, Canada.

Tomei, F. A., Barton, L. L., Lemanski, C. L., Zocco, T. G., Fink, N. H., Sillerud, L. O., 1995. Transformation of selenate and selenite to elemental selenium by *Desulfovibrio desulfuricans*. *Journal of Industrial Microbiology*, 14(3-4), 329-336.

Scheible, O., M. Mulbarger, P. Sutton, T. Simpkin, G. Daigger, J. Heidman, M. Yoder, D. Schwinn, D. Storrier, (1993). Process design manual: nitrogen control. EPA/625/R-93/010 (NTIS PB94159142), 1993.

US EPA., 1998. Method 6020A (SW-846): Inductively Coupled Plasma-Mass Spectrometry, Revision 1.

US EPA., 1994. Method 200.8: Determination of trace elements in waters and

943 wastes by inductively coupled plasma-mass spectrometry. Revision 5.4.
944 Cincinnati, OH.
945 US EPA., 2009. National Primary Drinking Water Regulations. EPA.816-F-09-004,
946 May 2009. https://www.epa.gov/ground-water-and-drinking-water/national-
947 primary-drinking-water-regulation-table
948 Vogel, M., Fischer, S., Maffert, A., Hübner, R., Scheinost, A. C., Franzen, C.,
949 Steudtner, R., 2018. Biotransformation and detoxification of selenite by microbial
950 biogenesis of selenium-sulfur nanoparticles. *Journal of Hazardous Materials*, 344,
951 749-757.
952 Wellen, C. C., Shatilla, N. J., Carey, S. K., 2015. Regional scale selenium loading
953 associated with surface coal mining, Elk Valley, British Columbia,
954 Canada. *Science of the Total Environment*, 532, 791-802.
955 Wozniak, B., Gerads, R., 2018. The role of speciation of selenium treatment and
956 compliance with site-specific aquatic life criteria. *Proceedings of Mine Water*
957 *Solutions,* 195-205.

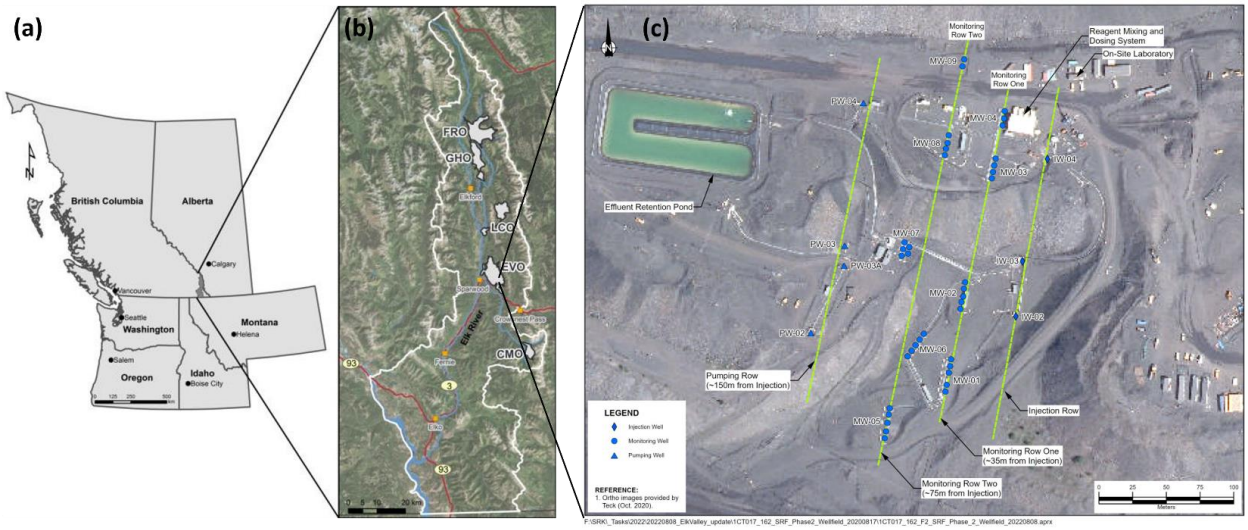

Figure 1. Location of Elk River Valley, British Columbia, Canada (a), regional coal mining operations (FRO, GHO, LCO, EVO, and CMO) in the Valley (b), and the locations of the injection, monitoring, and pumping wells in the SRF in (c) (from Hendry et al., 2023). In (b), the limits of the Elk River watershed boundary are delineated by a white line, the watercourses and lakes are indicated in blue, highways are indicated by red lines with numbers in yellow ovals, and individual coal mining operations are shaded in gray.

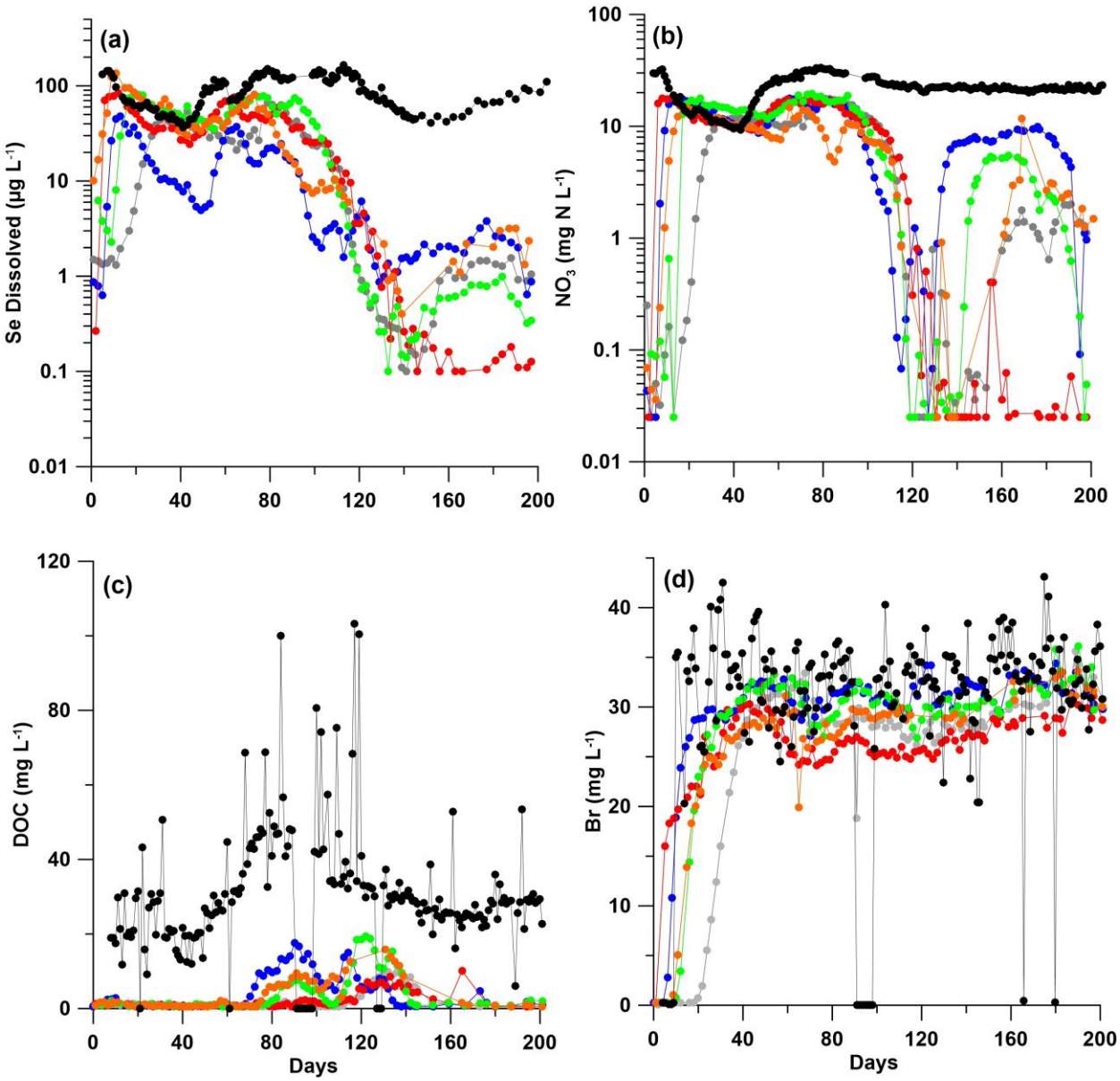

Figure 2. Concentrations of dissolved Se (a), NO_3^--N (b), methanol (as DOC) (c), and Br^- (d) from samples collected from injection wells (black) and monitoring wells 01A (gray), 02A (blue), 03A (red), 06A (green), and 07A (orange) vs. time since NO_3^- injection (day 1). Data for (b), (c), and (d) are from Hendry et al. (2023).

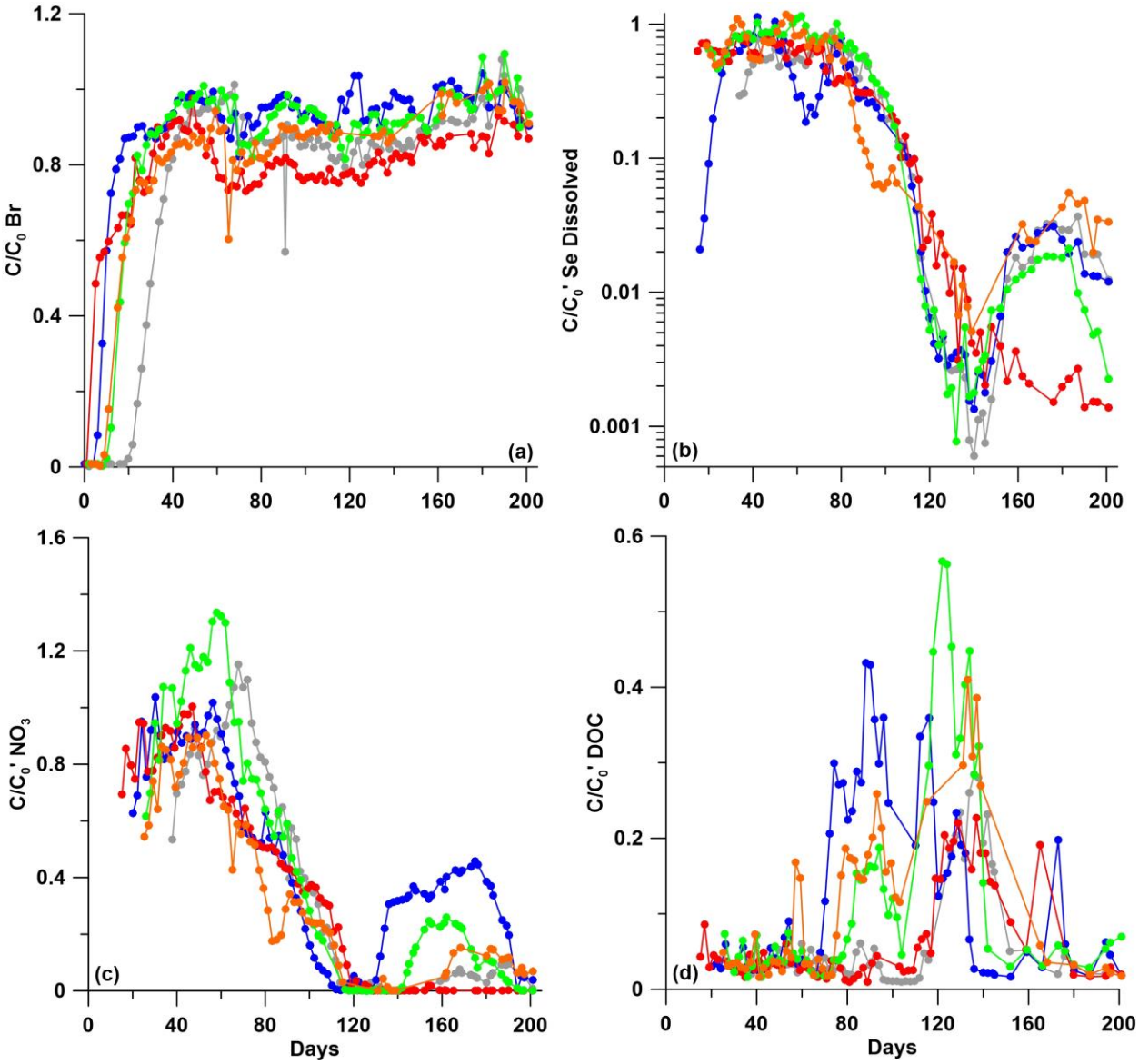

Figure 3. *C/C0* for Br^- (a) and *C/C0'* for dissolved Se (b), NO_3^- (c), and DOC (d) vs. time since NO_3^- injection (day 1) for monitoring wells 01A (gray), 02A (blue), 03A (red), 06A (green), and 07A (orange). Data for (a), (c), and (d) from Hendry et al. (2023).

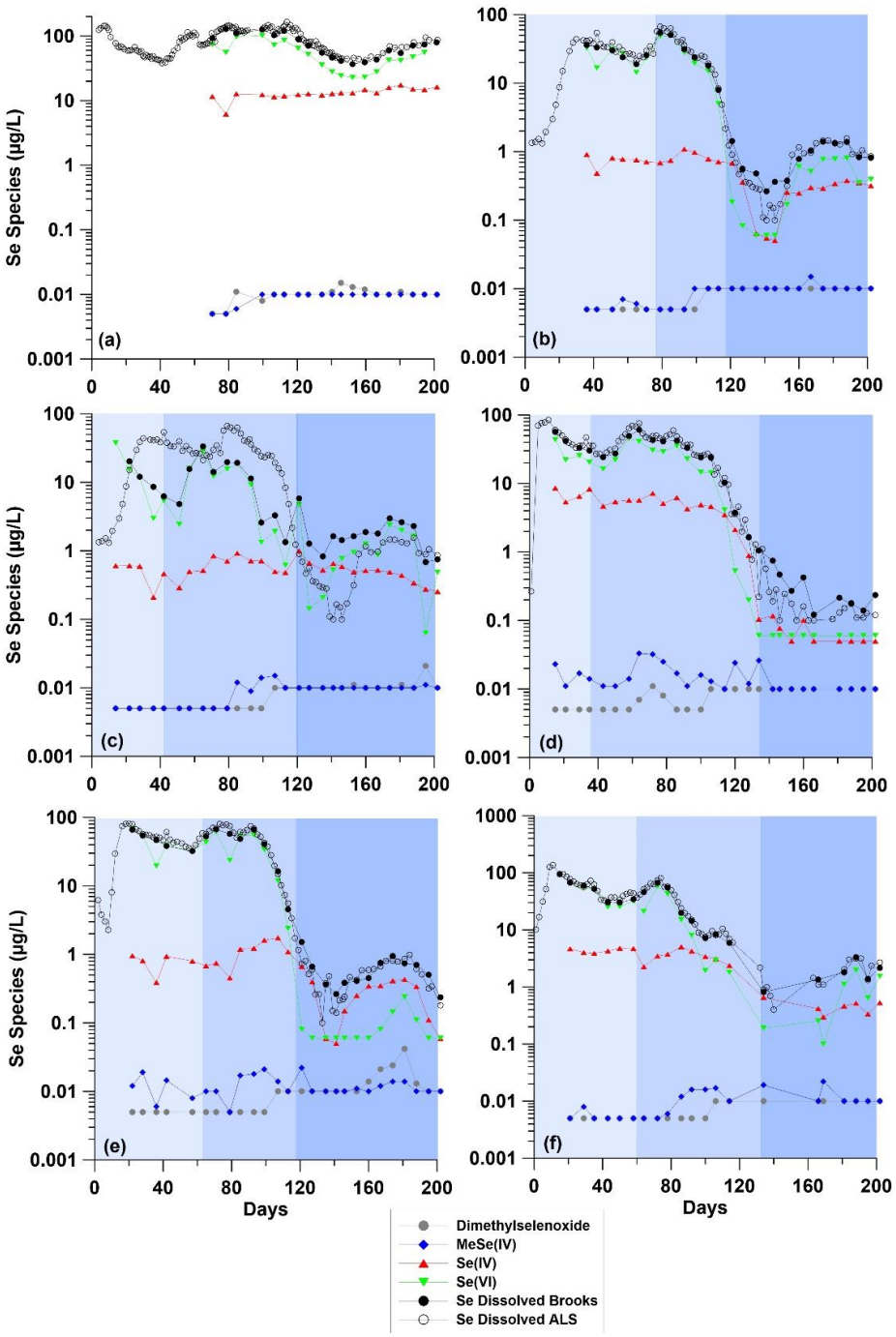

Figure 4. Measured Se species concentrations vs. time for injected water (a) and monitoring wells 01A (b), 02A (c), 03A (d), 06A (e), and 07A (f). Dissolved Se, Se(VI), and Se(IV) are represented by circles, squares, and diamonds, respectively. The dissolved Se data from ALS Environmental and Brooks Applied Labs are represented by open and solid circles, respectively. The colour bars delineate Zones 1, 2, and 3 from left to right, respectively. The boundaries between Zones 2 and 3 are defined as the day at which 99% Se reduction occurred.

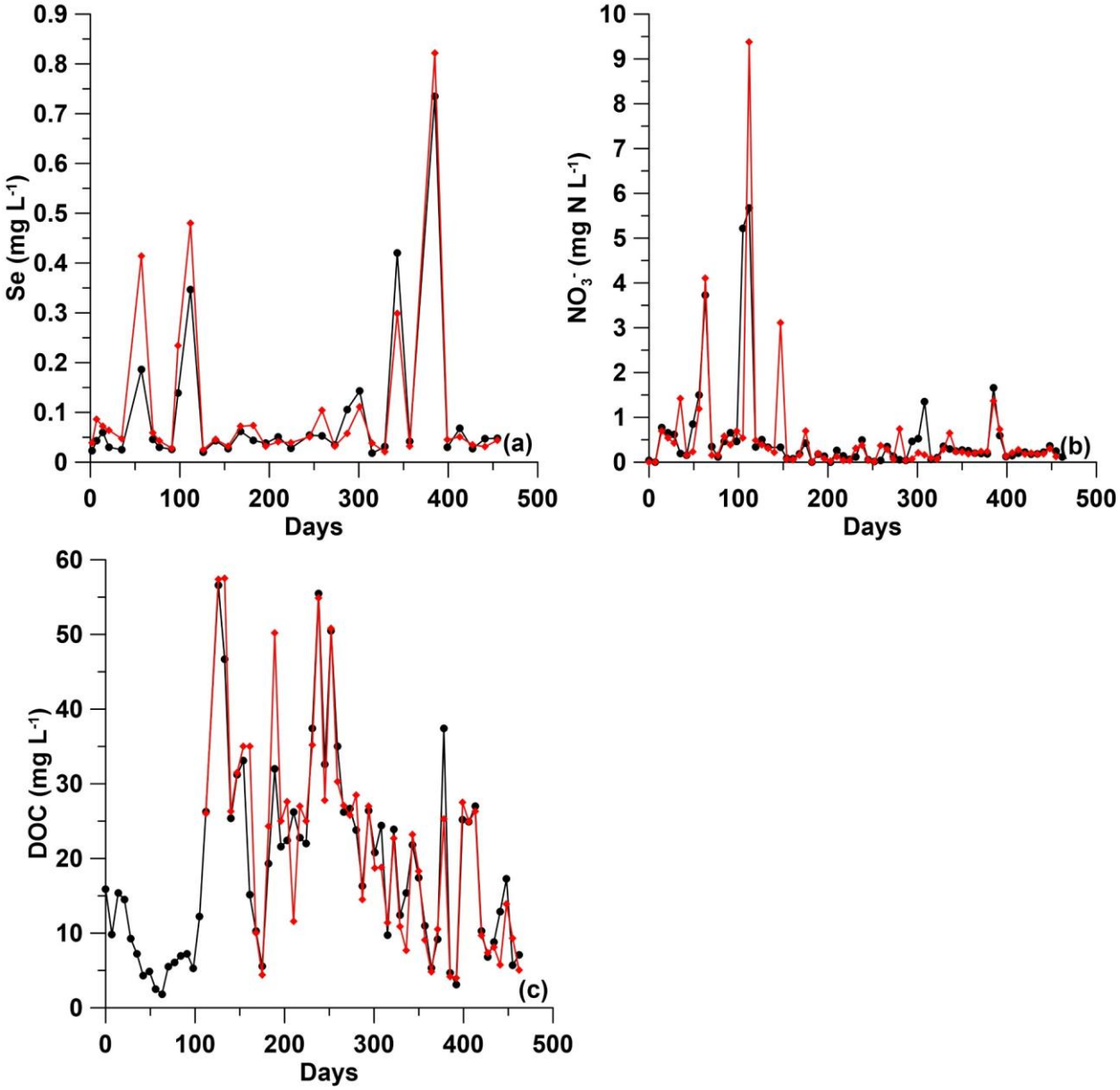

Figure 5. Measured dissolved Se (a), NO_3^--N (b), and DOC (c) concentrations vs. time in effluent water samples from columns 9 (black circles) and 10 (red diamonds). The dissolved Se, NO_3^--N, and DOC concentrations of the influent water were 1.0, 30, and 28.5 mg L^{-1}, respectively.

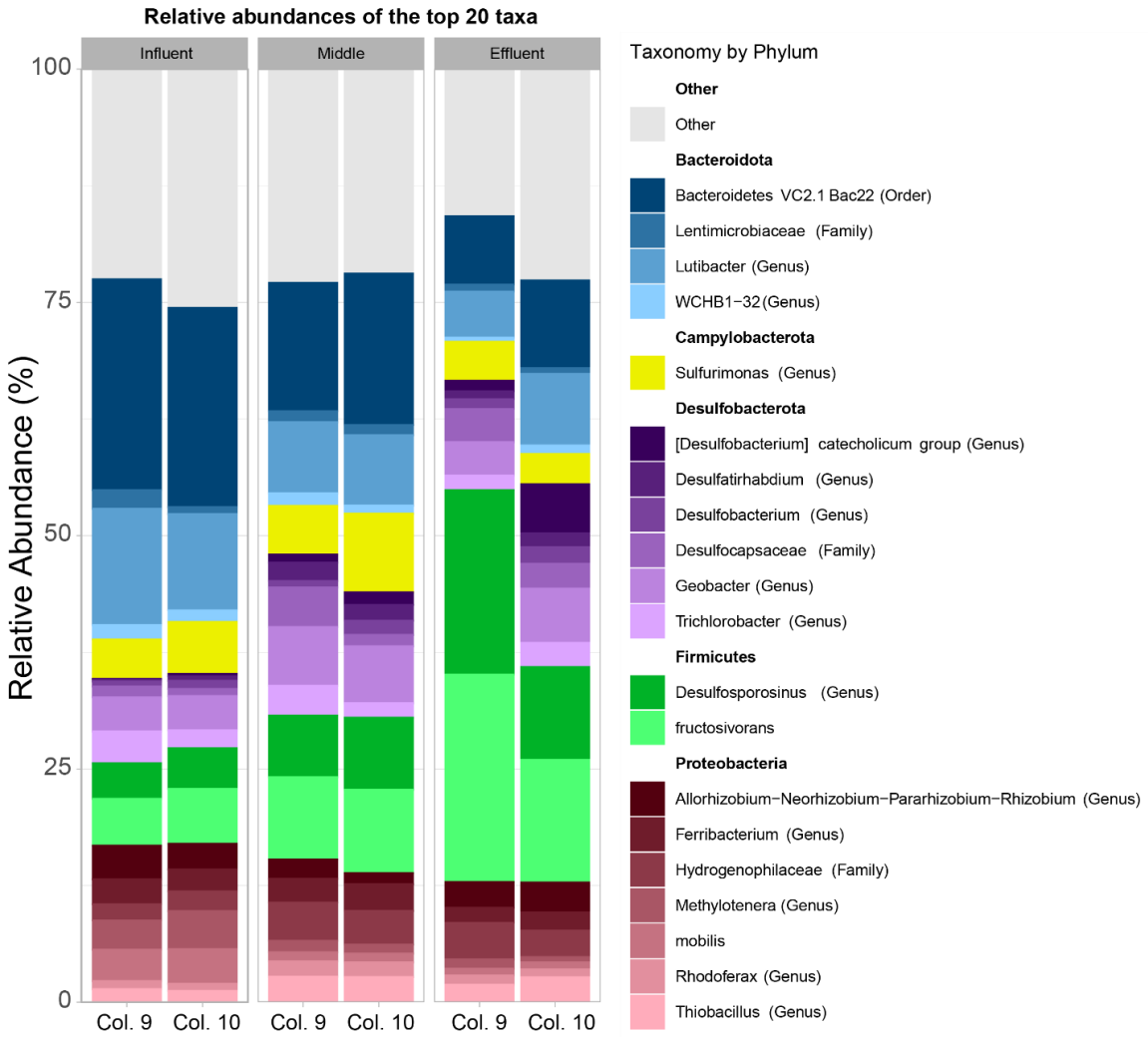

Figure 6. Microbial alpha diversity in columns 9 and 10. Comparison of the relative abundances of the 20 most abundant taxa detected at the influent (0 m), middle (0.1 m), and effluent (0.3 m) of columns 9 and 10. The taxa are represented by phylum and then as the highest resolution taxonomic level that could be classified, which is stated in parentheses if the taxon was not classified to the species level. All other taxa detected in the samples were grouped into the “Other” category.

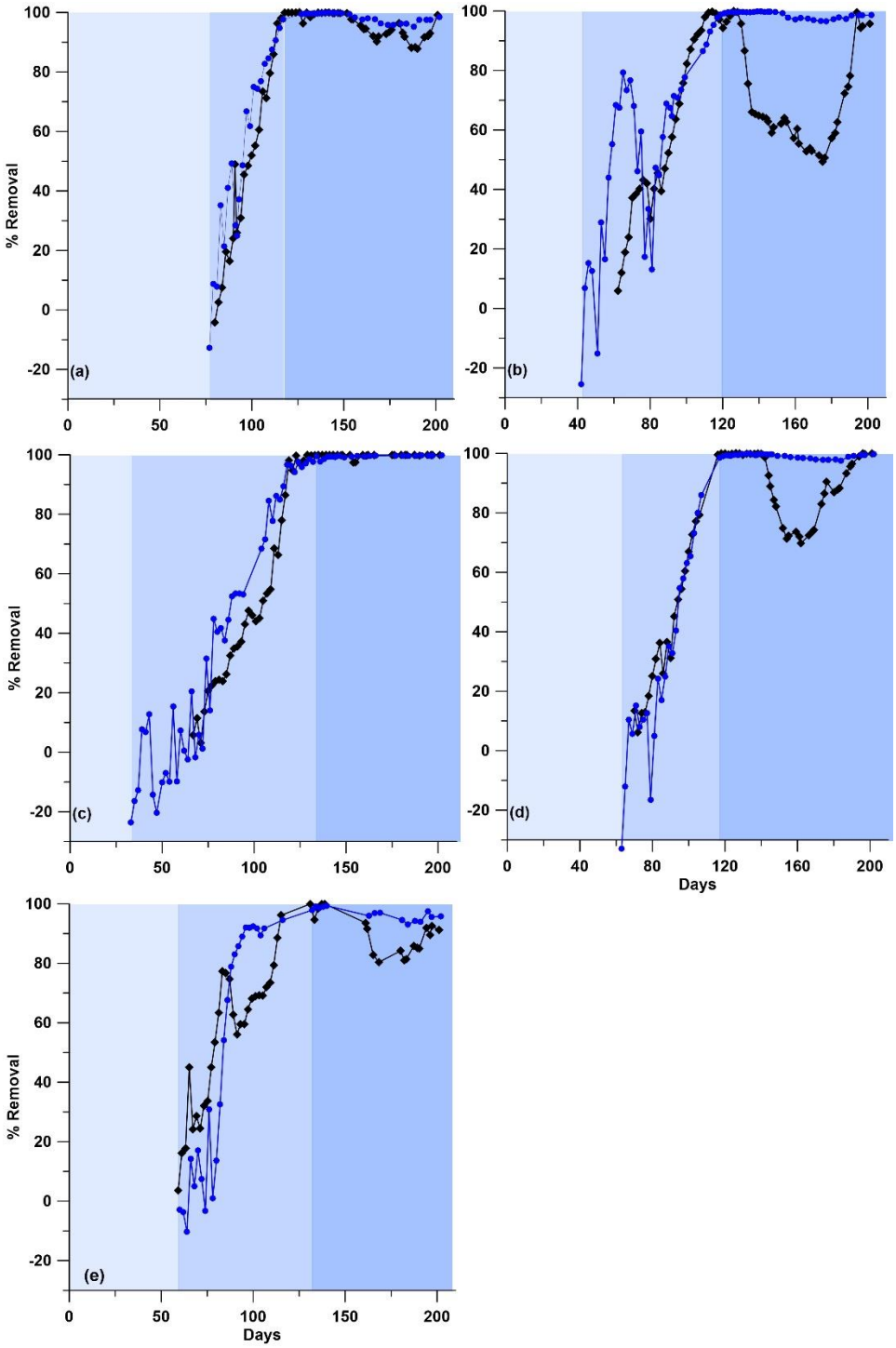

Figure 7. Calculated percent Se bioreduction (circles) and denitrification (diamonds) vs. time for monitoring wells 01A (a), 02A (b), 03A (c), 06A (d), and 07A (e) after the onset of Se reduction/denitrification. The colour bars delineate Zones 1, 2, and 3 from left to right, respectively. The boundaries between Zones 2 and 3 are from Figure 4. Percent denitrified data from Hendry et al. (2023).

Declaration of competing interest

The authors declare the following financial interests/personal relationships which may be considered as potential competing interests: Jim Hendry reports a relationship with Teck Resources Limited that includes: consulting or advisory. Lisa Kirk reports a relationship with Teck Resources Limited that includes: consulting or advisory. Jeff Warner reports a relationship with Teck Resources Limited that includes: consulting or advisory. Shannon Shaw reports a relationship with Teck Resources Limited that includes: consulting or advisory. Brent Peyton reports a relationship with Teck Resources Limited that includes: consulting or advisory. Erin Schmeling reports a relationship with Teck Resources Limited that includes: consulting or advisory. Lee Barbour reports a relationship with Teck Resources Limited that includes: consulting or advisory.

CRediT authorship contribution statement

M. Jim Hendry: Conceptualization, Methodology, Data curation, Writing – original draft, Writing – review & editing**. Lisa Kirk:** Methodology, Data curation, Writing – review & editing**. Jeff Warner:** Methodology, Data curation, Writing – review & editing**. Shannon Shaw**: Data curation, Writing – review & editing. **Brent M. Peyton**: Writing – review & editing. **Erin Schmeling**: Data curation, Writing – review & editing. **S. Lee Barbour**: Writing – review & editing.